An investigation on optical microfiber reflector with low reflectance

Yang Yu (于 洋), Xueliang Zhang (张学亮)*, Zhangqi Song (宋章启), Zhengtong Wei (卫正统), and Zhou Meng (孟 洲)

College of Optoelectronic Science and Engineering, National University of Defense Technology, Changsha 410073, China

**Corresponding author: xueliang.john@hotmail.com*

Received May 3, 2013; accepted November 28, 2013; posted online January 8, 2014

The backscattering characteristics of optical microfiber (OM) are experimentally studied by controlling heating temperature and cooling method during the OM fabrication process. OM samples with various reflectances from 0.1% to 1% are achieved. An OM with waist length of 5 mm, waist diameter of 1 μm, and approximately 0.5% reflectance is used as the end reflector of a fiber Fabry-Perol (F-P) interferometer. A piezoelectric ceramic transducer (PZT) fiber phase modulator is used to test the sensing performance of the fiber F-P interferometer. Experimental results verify that the OM with low reflectance can be used as a reflector in the F-P interferometer.

OCIS codes: 230.0230, 230.4000, 060.2370.
doi: 10.3788/COL201412.012301.

Optical microfiber (OM) has been widely studied for its special properties such as low transmission loss, large evanescent fields, high-nonlinearity, strong confinement, large waveguide dispersion, and small bending radius. It has potentially broad applications in photonic devices, such as optical sensing, nonlinear optics and quantum optics[1−9]. Numerous studies on the surface roughness of the OMs have been performed to obtain more perfect OMs with low loss, and this scattering has been considered one of the loss origins[10−15]. However, a detailed study on backscattering characteristics of OM has been rarely conducted. In this letter, the backscattering characteristics of the OM were experimentally studied by controlling heating temperature and cooling method during the OM fabrication process. Furthermore, an optical system was used to monitor the transmitted light and the backscattered light. An enhanced backscattering phenomenon in the OM was observed when adjusting the heating temperature and the cooling method in the OM fabrication process. Corresponding works on demonstrating the OM reflector with low reflectance were performed.

In order to analyze the backscattering characteristics of the OM, the backscattered light should be in *situ* detected during the OM fabricating process. Figure 1 shows the OM tapering device based on the modified flame-brushing technique[16], added with an in *situ* power detection system.

A telecom fiber (outer diameter 125 μm, numerical aperture 0.12) is clamped onto the two motorized precision translation stages and stretched under computer control, whereas the bare part of the fiber is heated by a microheater. Both stages and microheater are automatically controlled by a computer. One end of the drawn fiber is connected with a laser source (Agilent 8148A, output power 10 dBm) via an optical fiber circulator; the other end is directly connected to photodetector 1 (D1). The total power of the backscattered light along the fiber is measured through the optical fiber circulator by photodetector 2 (D2).

During the OM fabricating process, the softened OM may be affected by the air turbulence due to the moving OM in the surrounding air under the heating condition. At the end of the OM fabricating process, while we remove the microheater from the OM, the varying temperature field will affect the OM shape. Reference [15] has studied the surface non-uniformity of the OM waveguide in detail, which can lead to transmission loss. We attempted to vary the removing velocity of the microheater in our OM fabracation experiments, and found that the reflection light had increased correspondingly. We had attained tens of OM samples with 5-mm waist length and 2-μm waist diameter with the improved setup by increasing the microheater's temperature and removing the microheater from the OM quickly. When the microheater is removed, the backscattering light power will rise quickly, as shown in Fig. 2 (the quickly rising part is marked with a circle). The input laser power was approximately 10 dBm. Figure 2 indicates that the reflectance of the OM sample was approximately –30 dB, or expressed as 0.1%.

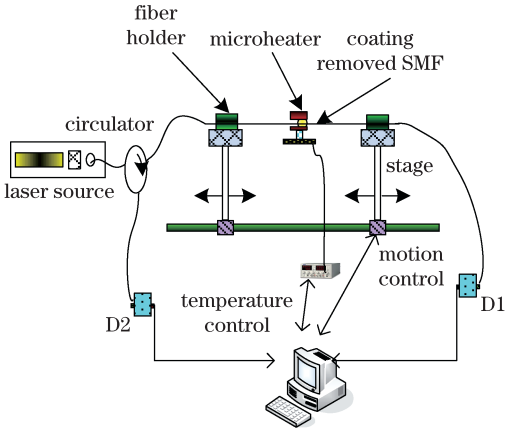

Fig. 1. Setup of OM fabrication with power monitoring system.

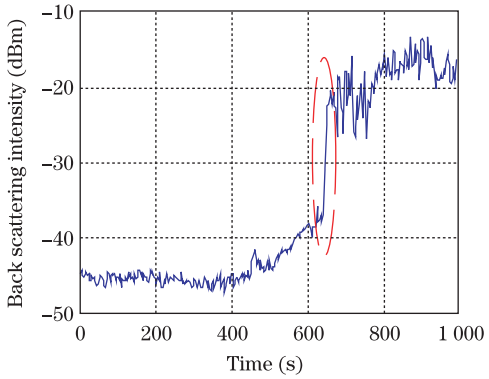

Fig. 2. (Color online) Backscattering light monitoring during the OM drawing process (the red circle marks the time when the microheater is removed).

We conducted numerous OM fabricating experiments to analyze the backscattering feature, and found that obvious increment of the power of the backscattered light occurred especially when the waist diameter of the OM was less than 4 μm. The backscattering of the OM was strongly affected by the microheater's temperature and the annealing time. The special OM fabrication technique with different backscattering levels was primarily realized in our lab by introducing the temperature feedback controlling technology in the OM fabricating system. The high backscattering OMs with waist length of several mm and waist diameter of less than 2 μm had been achieved, with various reflectances from 0.1% to 1%.

In order to explore the backscattering characteristics of the OMs, a distributed fiber backscattering analyzer (LUNA, OBR4600) was used to measure an OM with waist length of 5 mm and waist diameter of 2 μm. The OM was connected with OBR4600 by an approximately 4-m fiber pigtail, and an approximately 2-m fiber pigtail at the other end of the OM. The measured results are shown in Figs. 3(a) and (b). The resolution of the OBR4600 analyzer was set as 50 μm in the experiment.

In Fig. 3(a), A and C are due to reflections of the two ends of the OM pigtails, B is due to the backscattering of the OM region, which is identified following the total fiber sample length. The B point is magnified and plotted in Fig. 3(b). D is a joint of the fiber sample. The part after C is the noise floor of the device. The part between A and B is the distributed backscattering power of the conventional fiber pigtail before the OM region, showing that the relative backscattering power value is approximately –120 dB. At the 4352-mm place shown in Fig. 3(b), the highest relative backscattering power value due to a point in the OM region is approximately –56 dB. Notably, the highest backscattering power in the OM is almost 64 dB higher than that of the conventional fiber. Based on Fig. 3(b), the backscattering power increases from the taper region of the OM to the waist region, and reaches the highest in the middle of the OM region. The majority of the backscattering power is from the 5-mm waist region of the OM. Thus, this type of OM sample can be used as a reflector with low reflectance.

In order to identify the nature of the backscattered light in the OM, we also measured the amplified backscattering light from the OM with an optical spectrum analyzer (OSA). The measured spectrum indicates no other new spectrum line but the original peak, showing that no stimulated Raman scattering or stimulated Brillion scattering or any other stimulated Rayleigh scattering occurs. We believe that the OM is perturbed at the end of drawing process. Although the microheater is removed quickly, it may change the structure of the cylindrical optical waveguide at the subwavelength scale, appearing as microstructures in the OM and surface non-uniformity of the OM waveguide[17].

Although the reflectance of the OMs is weak, the OMs may be used as reflectors in certain fiber sensing systems, such as Fabry-Perol (F-P) sensor.

An OM with waist length of 5 mm, waist diameter of 1 μm, and approximately 0.5% reflectance was prepared and used as an end reflector in an F-P interferometer, shown in Fig 4. The front reflector was realized using the end face of a physical contact (PC), which indicated reflectance of approximately 0.1%. Between the two reflectors, a piezoelectricity transducer (PZT) fiber phase modulator was used to produce analog signal in the F-P interferometer. The total fiber length between the two reflectors is 5 m. Thus, a high coherence laser source (RIO company's source with 1550-nm wavelength, and line width of approximately 3 kHz) was selected as the light source of this interferometer and digital phase generation carrier (PGC) with light source frequency modulation was used to demodulate the signal produced by the PZT fiber phase modulator.

An optical fiber circulator was used to lead the reflected light into a photodetector. A computer with PGC

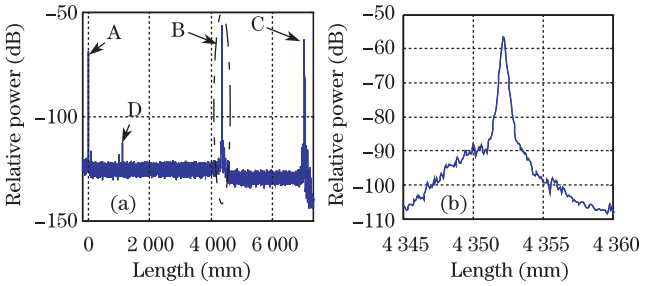

Fig. 3. (a) Backscattering of OM measured with an OBR4000 analyzer (OM waist length of 5 mm, OM waist diameter of 2 μm). (b) Local magnifying plot of B in Fig. 3(a).

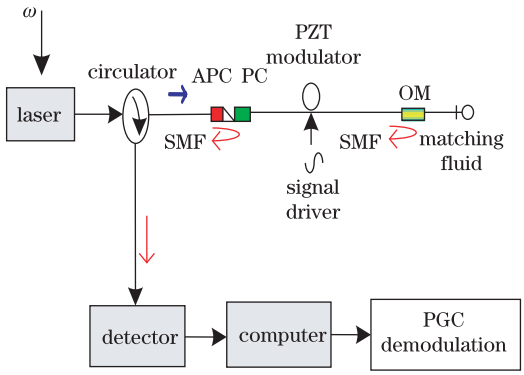

Fig. 4. A F-P interferometer sensing system with OM as the end reflector. "PC" represents a physical contact and "APC" is an angled physical contact.

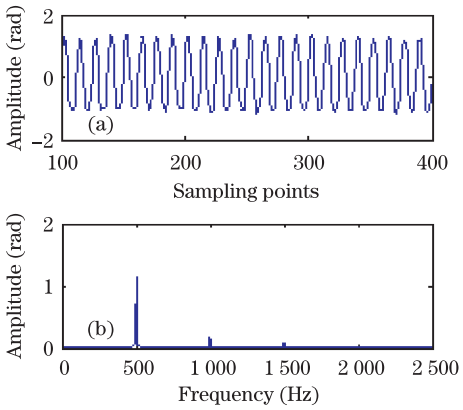

Fig. 5. F-P sensing system output signal in (a) time domain and (b) frequency domain, when the PZT modulator is applied with signal with 500-Hz frequency and 1-V amplitude.

demodulating software was used to calculate and output the demodulating result. The output signal of the photodetector is[18]

$$V = A + B\cos[C\cos\omega_0 t + \varphi_s(t) + \varphi_0], \qquad (1)$$

where C is the modulating depth, ω_0 is the modulating angular frequency, A is the DC term related to optical power, B is the amplitude related to the interferometer visibility, φ_s(t) is the analog signal produced with the PZT fiber phase modulator and φ_0 is the initial phase. For the detailed PGC demodulating method of the F-P double beam interferometer, please refer to the Michelson-interferometer in Ref. [18].

By choosing proper modulating depth C and other parameters, the interferometer outputs a steady demodulated signal[18]. In our experiment, the modulating frequency of the signal on the RIO laser is 6.25 kHz, the modulating amplitude is 0.5 V. In fact, we may deduce the fiber length between the PC reflector and the OM reflector based on the proper C value for a determined RIO laser.

When we added signal with amplitude at approximately 1 V and frequency from 200 to 2000 Hz, the F-P sensing system outputs corresponding frequency signals. The output phase signal (unit: rad), which is demodulated from the output signal of the photodetector, is shown as Fig. 5, when the PZT modulator was applied with signal with 500-Hz frequency and 1-V amplitude.

After the experiments, we damaged the OM reflector and noticed that the F-P sensing system stopped working. The above results show that the OMs can be used as reflectors with low reflectance in F-P interferometers.

In conclusion, with proper control method, OM samples with various backscattering characteristics can be achieved in our setup. We analyze the backscattering characteristics experimentally and find that a clear back reflection effect occurres at the OM region. A fiber F-P interferometer is set up with an OM sample as the end reflector. Corresponding experimental results show that the OM actes as an effective reflector. The OMs with enhanced backscattering effect may be useful in certain fiber sensing systems. Further works will focus on the mechanism and accurate control of OM reflectance.

References

1. L. Tong, F. Zi, X. Guo, and J. Lou, Opt. Commun. **285,** 4641 (2012).
2. G. Brambilla, F. Xu, P. Horak, and Y. Jung, Advances in Optics and Photonics **1,** 107 (2009).
3. G. Brambilla, Opt. Lett. **12,** 043001 (2010).
4. G. Brambilla, Opt. Fiber Technol. **16,** 331 (2010).
5. L. Tong, F. Zi, X. Guo, and J. Lou, Opt. Commun. **285,** 4641 (2012).
6. J. Fu, X. Yin, N. Li, and L. Tong, Chin. Opt. Lett. 6, 112 (2008).
7. F. Tian, G. Yang, J. Bai, Q. Zhou, C. Hou, J. Xu, and Y. Liang, Chin. Opt. Lett. **8,** 326 (2010).
8. X. Kou, G. Vienne, and G. Wang, Chin. Opt. Lett. **8,** 560 (2010).
9. Z. Wei, Z. Song, X. Zhang, and Z. Meng, Chin. Opt. Lett. **11,** 1671 (2013).
10. J. Jäkle and K. Kawasaki, J. Phys. Condensed Matter **7,** 4351 (1995).
11. M. Sumetsky, Y. Dulashko, J. M. Fini, A. Hale, and J. W. Nicholson, Opt. Lett. **31,** 2393 (2006).
12. M. Sumetsky, Opt. Express **15,** 1480 (2007).
13. G. Zhai and L. Tong, Opt. Express **15,** 13805 (2007).
14. A. V. Kovalenko, V. N. Kurashov, and V. Kisil, Opt. Express **16,** 5797 (2008).
15. L. Tong and M. Sumetsky, *Subwavelength and Nanometer Diameter Optical Fibers* (Springer, 2009).
16. G. Brambilla, F. Xu, and X. Feng, Electron. Lett. **42,** 517 (2006).
17. S. Sakaguchi, J. Lightwave Technol. **11,** 187 (1993).
18. X. Zhang, Z. Meng, Z. Hu, H. Yang, Z. Song, and Y. Hu, Proc. SPIE **7278,** 72781N (2008).